vibration

MDPI

Article

Nonlinear Piezoelectric Energy Harvester: Experimental Output Power Mapping

Ioan Burda

Physics Department, Babes-Bolyai University, 400084 Cluj-Napoca, Romania; ioan.burda@ubbcluj.ro

Abstract: In this paper, the output power map of a nonlinear energy harvester (PEH) made of a console beam and the membrane of a resonant vibration speaker is analyzed experimentally. The PEH uses two large piezoelectric patches (PZT-5H) bonded into a parallel bimorph configuration. The nonlinear response of the deformable structure provides a wider bandwidth in which power can be harvested, compensating for the mistuning effect of linear counterparts. The nonlinear response of the proposed PEH is analyzed from the perspective of its electrical performance. The proposed experimental method provides novelty by measuring the effects produced by the nonlinearity of the deformable structure on the output power map. The objective of this analysis is to optimize the size of the PZT patch in relation to the size of the console beam, providing experimental support for the design. The presentation of the most significant experimental results of a nonlinear PEH, followed by experimental mapping of the output power, ensured that the proposed objective was achieved. The accuracy of the experimental results was determined by the high degree of automation in the experimental setup, assisted by advanced data processing.

Keywords: piezoelectric energy harvester; nonlinear; piezoelectric materials; cantilever beam

Citation: Burda, I. Nonlinear Piezoelectric Energy Harvester: Experimental Output Power Mapping. *Vibration* **2022**, *5*, 483–496. https://doi.org/10.3390/vibration5030027

Academic Editors: Kai Zhou, Hongling Ye, Qi Shuai and Aleksandar Pavic

Received: 22 June 2022
Accepted: 25 July 2022
Published: 27 July 2022

1. Introduction

Piezoelectric energy harvesting is the process by which mechanical vibration energy is extracted from ambient sources and converted into electrical energy [1,2]. This form of ambient energy is abundant in the environment, and this motivates its widespread exploitation [3,4]. A piezoelectric harvester exploits a deformable structure subjected to ambient mechanical vibrations to induce stress/strain in a piezoelectric layer glued to it [5,6]. By reducing the power consumed by modern electronic devices, the nonlinear piezoelectric energy harvester (PEH) is given the chance to contribute to the realization of self-powered versions [7–9].

In the case of a deformable structure with linear frequency response, the harvested power decreases rapidly if the frequency of ambient mechanical vibrations differs by more than 1–2% of its natural resonant frequency. The higher the quality factor (Q) of the linear deformable structure, the less robust the PEH is. Because of this, the linear PEH is complicated to manufacture based on matching the natural resonance frequencies of the deformable structure [10] with the frequencies of the ambient mechanical vibrations. The decrease in the natural resonance frequency of the deformable structure causes a decrease in the recovered energy, so the efficient harvesting of low-frequency vibrations remains a challenge [11,12].

Deformable nonlinear structures have attracted many research efforts, emphasizing their advantages for the realization of an energy harvesting device [13,14]. In this regard, the use of Duffing oscillators as mono-stable harvesters or different versions of bi-stable or multi-stable harvesters has been studied by several authors [15,16]. A Duffing oscillator is usually materialized as a piezo–magneto–elastic structure composed of a console beam, with permanent magnets intentionally used to produce two potential energies [17–19]. A nonlinear energy harvester was analyzed, taking into account the softening or hardening

responses [20]. A nonlinear PEH consisting of bi-stable composite arrangements combined with piezoelectric elements ensures the harvesting of energy from ambient vibrations in a wide bandwidth [21].

More recently, new deformable structures have been proposed for nonlinear PEHs, and the advantages of these approaches are demonstrated theoretically and experimentally [22]. Deformable composite structures with an internal resonance response [23–25] complete the scope, and there has recently been a tendency to unify PEH modeling [26,27]. In addition, the use of piezoelectric transducers offers several advantages compared to other methods of converting mechanical vibration energy into electrical energy [28]. The main advantage is the possibility of their use in magnetic environments and the high electromechanical coupling compared to that of the electromagnetic energy harvesters [29]. Piezoelectric energy harvesters also have the advantage of scalability and feasible implementation at micro or nano sizes [30,31].

The main novelty of the present paper is the experiential measurement of the output power maps to optimize the design of the harvester. Understanding and controlling nonlinear deformable structures are vital for applications [32,33], and the experimental measurement of the output power map provides detailed information on how energy is transferred from the nonlinear deformable structure to the attached piezoelectric patches.

This paper is organized as follows: Section 2 gives a brief introduction to the theoretical aspects of nonlinear PEH and describes an experimental nonlinear deformable structure. The section ends with a presentation of the experimental setup, largely automated. Section 3 presents significant results that describe the behavior of the nonlinear PEH and experimental mapping of the output power. Section 4 discusses the experimental results of the proposed nonlinear PEH response analyzed in terms of its electrical performance. Finally, Section 5 concludes the paper.

2. Materials and Methods

2.1. Basic Principles of the Nonlinear Piezoelectric Energy Harvester

Piezoelectric energy harvesting devices based on deformable linear structures operate in a narrow frequency band. A linear PEH is a resonant system that can be described by a second-order differential equation with a single degree of freedom. The differential equation of motion is given by [9]:

$$m\ddot{z} + d\dot{z} + kz = -m\ddot{y}, \tag{1}$$

where $y(t) = Ycos(\omega t)$ is the displacement of the vibration source, m is the effective mass, $z(t)$ is the relative displacement between the vibrating mass and the vibration source, k is the rigidity of the deformable structures, d is the damping coefficient and ω is the excitation frequency. Unlike the ideal linear case, in reality, non-linearities are present in deformable structures due to the geometric properties and/or materials involved. In general, these non-linearities have a very low impact on linear PEH. The intentional introduction of nonlinearities into PEH by external means [34] favors the process of converting the energy of the mechanical vibrations into electrical energy. The nonlinearity effect is generated by the introduction of a nonlinear restoration force whose magnitude and nature can be controlled [35]. For a nonlinear system, the equation of motion, Equation (1), is replaced by the Duffing equation written in the following form [9]:

$$m\ddot{z} + d\dot{z} + f(z) = -m\ddot{y}, \tag{2}$$

where $f(z)$ is the restoring force in the form of a combination of linear k and nonlinear stiffness $k_n z^2$ given by:

$$f(z) = \left(-k + k_n z^2\right) z, \tag{3}$$

In Equation (3), for $k_n \neq 0$, the total stiffness of the system is a function of z^2. Therefore, the total stiffness of the deformable structure would become harder for $k_n > 0$

and softer for $k_n < 0$. Consequently, in the particular case of a nonlinear PEH, the restoring force is dependent on the amplitude of mechanical vibrations in the deformable structure.

The linear PEH according to Equation (3) is described by the particular case where $k \leq 0$ and $k_n = 0$. In general, based on Equation (3), three nonlinear situations can be identified and are described below. Two iconic responses of nonlinear deformable structures described above, depending on the forcing frequency, are shown in Figure 1. The nonlinear stiffness $k_n < 0$ causes a softening response, and the frequency response of the deformable structure would bend to the left, as is shown in Figure 1a. This situation occurs only when sweeping is done from frequencies higher than the resonant frequency to lower frequencies.

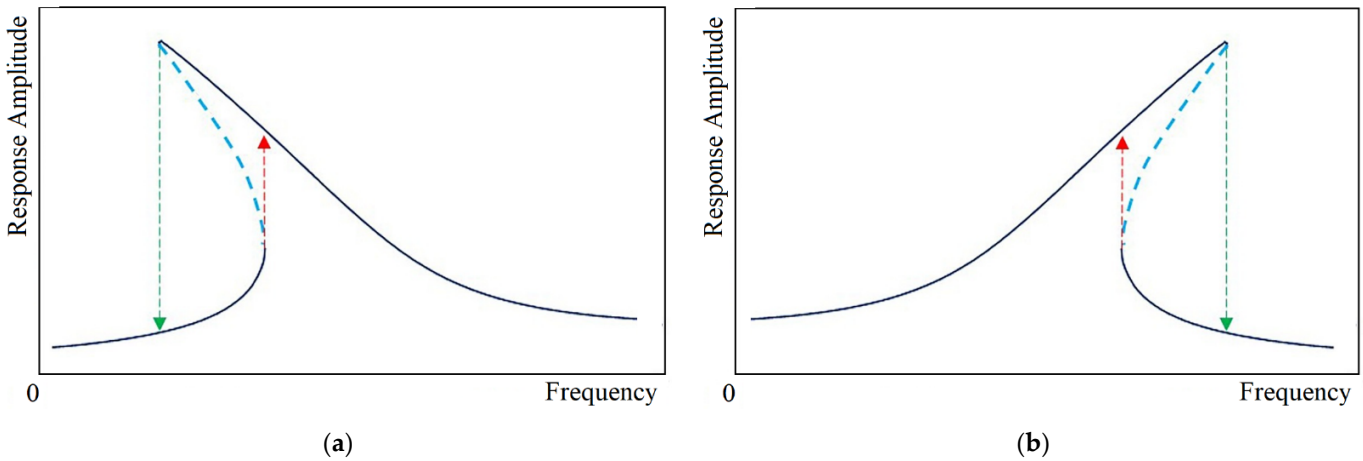

Figure 1. Frequency response curves of the nonlinear deformable structure: (**a**) softening effect with the jumps and frequency sweep direction indicated by arrows, (**b**) hardening effect with the jumps and frequency sweep direction indicated by arrows.

For $k < 0$, the system response is mono-stable. A nonlinear stiffness, $k_n > 0$ causes a hardening response, and the frequency response of the deformable structure would bend to the right, as is shown in Figure 1b. However, this only happens when the deformable structure is excited from frequencies lower than the resonant frequency [2] to higher frequencies.

For $k > 0$ and $k_n > 0$, the system becomes bi-stable and, in this case, the oscillation depends on the amplitude of the excitation. For a low excitation amplitude, the system behaves as a mono-stable system with a softening response. As the amplitude of excitation is increased above a certain level, the system begins to show aperiodic or chaotic oscillations. To create nonlinear PEH, most of the existing literature exploits magnetic interactions [36,37] to create magnetically bi-stable deformable structures. Other approaches include the use of nonlinear springs [38] and the use of amplitude limiters [30] to create mechanically bi-stable deformable structures. For both stiffness softening and hardening, as is shown in Figure 1, a wider frequency bandwidth occurs, but this depends on the frequency sweep directions. It is also possible to have a multi-stable system with more than two equilibrium points [39]. The presence of multi-stable positions implies a system response dependent on the amplitude of mechanical vibrations [40,41].

2.2. Mechanical Setup

In this study, the nonlinear response of a deformable structure was exploited. The main components of the deformable structure were a console beam covered with two piezoceramic patches, PZT-5H, and the membrane of a resonated vibration speaker. A diagram of the mechanical setup, including fasteners and a piezoelectric accelerometer B&K 4383 (Brüel & Kjær, Nærum, Denmark), is shown in Figure 2.

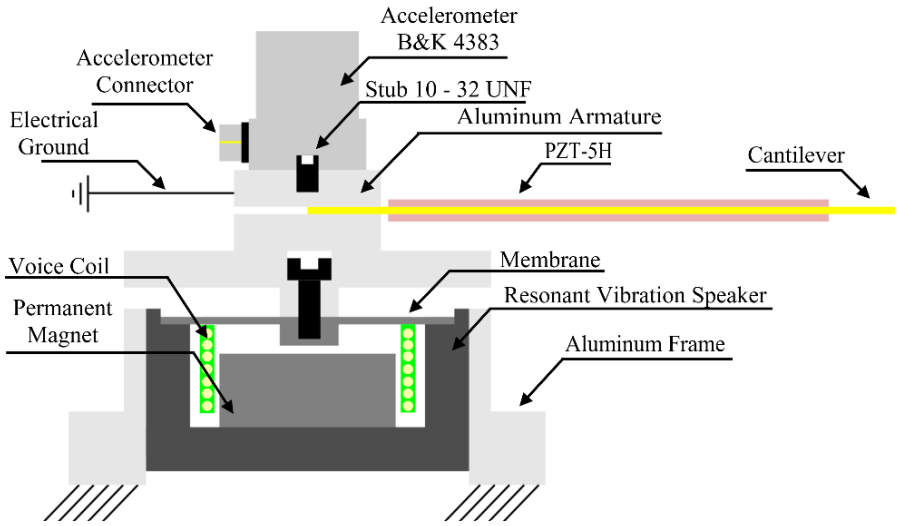

Figure 2. Mechanical setup of the nonlinear piezoelectric energy harvester.

The resonant vibration speaker with a rated power of 20 W and an impedance of 4 Ω measured at 1 kHz (Dongguan QianYin Electroacoustic Co., Ltd., Dongguan city, China) is used as a source of vibration, and its membrane is part of the deformable structure. The resistance of the voice coil from Figure 3a is equal to 3 Ω and the inductance is 0.159 mH.

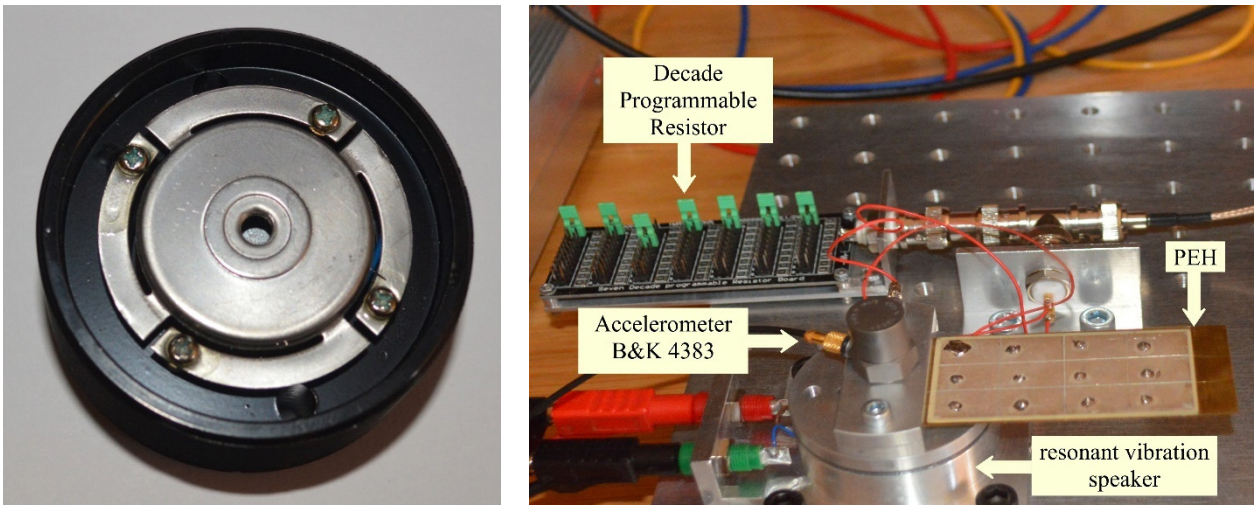

(**a**) (**b**)

Figure 3. Mechanical setup: (**a**) the resonant vibration speaker; (**b**) the mechanical setup assembled with PEH prepared for measuring the output power map.

The mechanical device consisted of an aluminum frame that provided a rigid fixation to an optical table as is shown in Figure 3b. The experimental results largely depended on the quality of the mechanical setup. For this reason, its design and manufacture had to ensure the robustness necessary for a stable behavior.

A nonlinear PEH made in a parallel bimorph configuration was used in the investigations as two independent PZTs with common ground. One PZT was used to experimentally measure the electrical performance of the PEH and the other PZT was prepared to measure the output power map. The size of the brass cantilever was 80 mm × 33 mm × 0.2 mm and on the two sides were glued to two PZT-5H patches with a size of 60 mm × 30 mm × 0.2 mm (Sunny Electronics Technology Co., Ltd., Suzhou, China). The mechanical parts of the deformable structure were connected in a series.

2.3. Experimental Setup

In Figure 4a, the experimental setup is presented as a diagram of electrical connections. Additional equipment was connected to a laptop PC to do data acquisitions through USB interfaces using Matlab® scripts (The MathWorks, Inc., Natick, MA, USA). An overview of the experimental setup is illustrated in Figure 4b, where the equipment involved is highlighted.

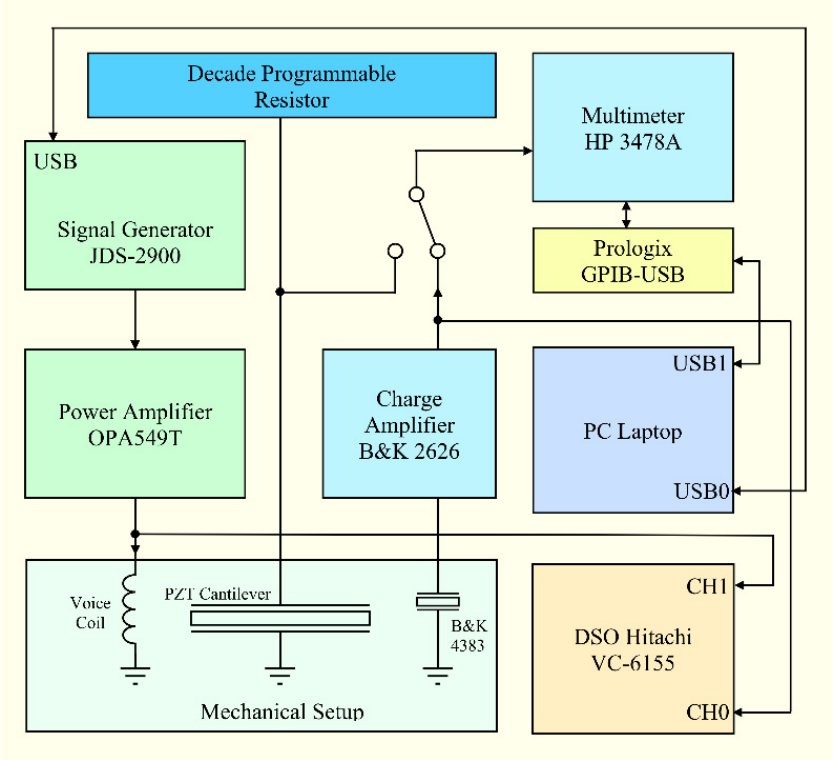

(**a**)

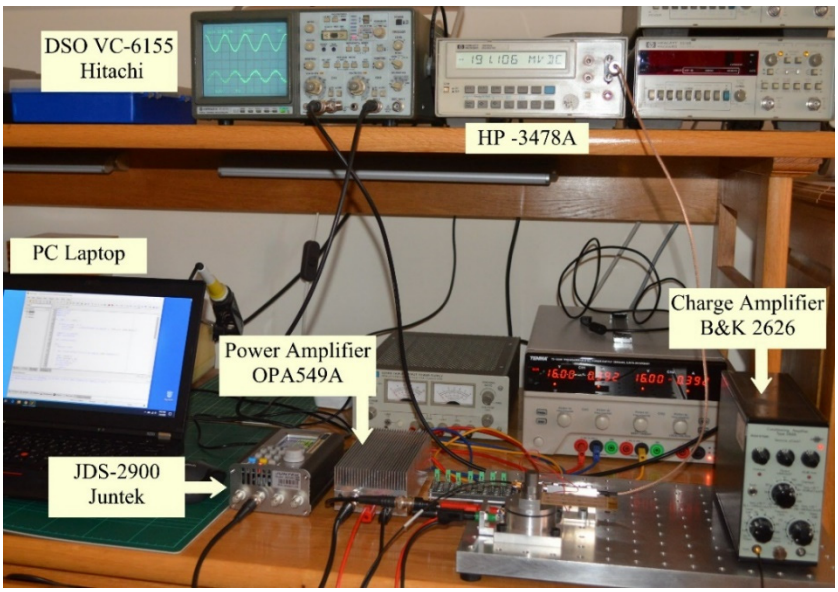

(**b**)

Figure 4. Experimental setup: (**a**) block diagram and (**b**) equipment involved.

The electrical performance of a nonlinear PEH was investigated in an automated experimental setup. The equipment included (i) a signal generator JDS-2900 (Juntek, Co., Ltd., Shanghai, China) followed by a high-power amplifier (OPA549, Texas Instruments, Inc.,

Dallas, TX, USA) to control the vibration source, (ii) a decade programmable resistor, and (iii) an HP-3478A multimeter with the input impedance of 1 MΩ parallel to the less than 60 pF (Agilent Technologies, Inc., Santa Clara, CA, USA) used to measure the true root mean square (rms) of the output AC voltage of the nonlinear PEH. The amplitude of the vibration was supervised by accelerometer B&K 4383 followed by the charge amplifier B&K 2626 (Brüel & Kjær, Nærum, Denmark). A digital storage oscilloscope VC-6155 (Hitachi Ltd., Tokyo, Japan) was used to monitor the sinusoidal voltage at the output of the power amplifier and the output of the B&K 2626 charge amplifier. The sound card of the PC laptop was used to acquire the signal from the output of the aforementioned charge amplifier.

3. Results

3.1. Dynamic Characterization of the Nonlinear Piezoelectric Energy Harvester

The first investigation was performed on the vibration source in the frequency range used to investigate the PEH. These measurements were conducted without a PEH to avoid any external perturbation induced by the cantilever beam. The relationship between the frequency and acceleration (the amplitude of the sinusoidal wave) is shown in Figure 5.

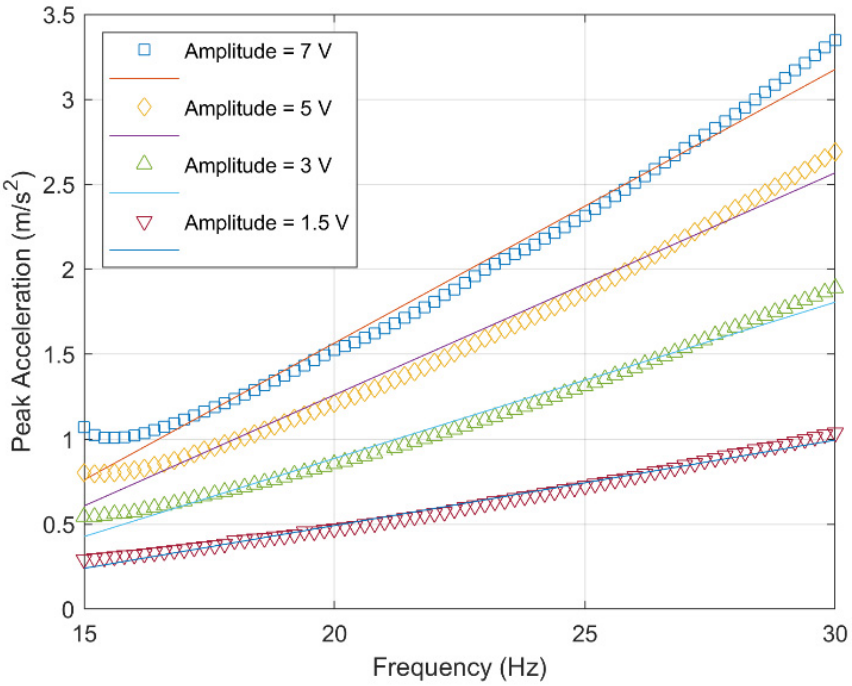

Figure 5. The frequency–acceleration response to the excitation of the resonant vibration speaker in the range of 15–30 Hz for several values of the sinusoidal wave amplitude.

The previous calibration measurement was carried out with professional-grade equipment, as shown in Section 2. Each point was obtained in steady-state conditions. The optimal data acquisition time was determined by the constant value of the measured voltage. The range of acceleration peaks used in the PEH investigation was from 0.25 m/s^2 to 3.4 m/s^2. For the investigated frequency range, the frequency response was linear, as shown in Figure 5, with a linear fit. The impedance of the resonant vibration speaker in the investigated frequency range changed by only 0.015 Ω. The behavior shown in Figure 5 is determined by the frequency response characterized by a steep roll-off towards low frequencies.

To simplify the procedures of the experiment and to provide a clearer picture of the nonlinear PEH behavior from the perspective of electrical properties, the frequency of response of the function (FRF) is presented according to the amplitude of the sinusoidal wave used for excitation.

Both softening stiffness and hardening were encountered in the deformable structure investigated, and the behavior depended on the amplitude of sinusoidal excitation. For this research, only the hardening response was retained due to the high deformation of the free end of the console beam. This response significantly amplified the vibrational amplitude and ensured the generation of stress/strain for the piezoelectric effect, which led to higher output energy. Nonlinear behavior of the deformable structure was demonstrated for the amplitudes of the sinusoidal waves that produced a peak-to-peak vibration at the free end of the cantilever beam of 7 mm. The up and down frequency sweep determines the open-circuit voltage response to the vibrations induced in the PEH, as shown in Figure 6.

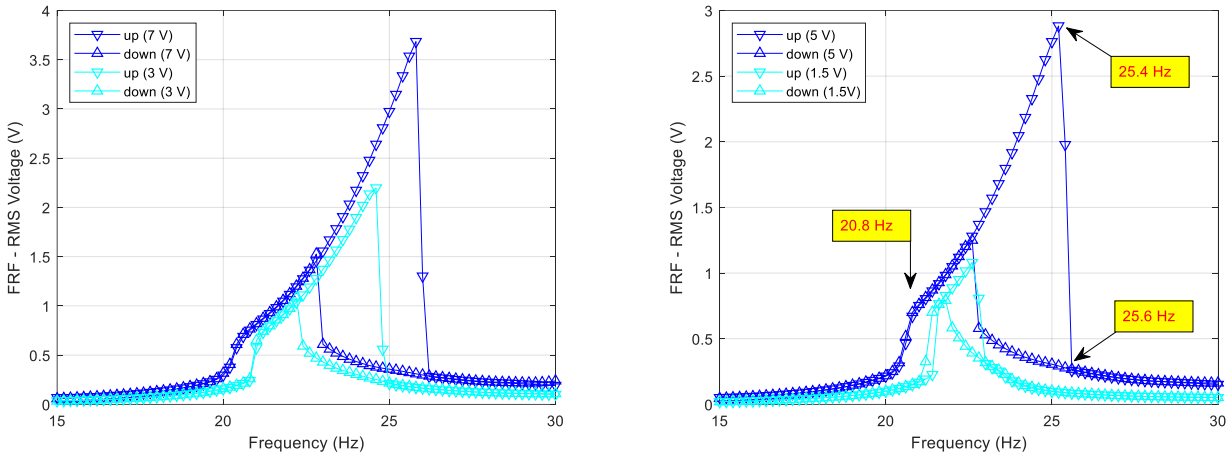

(**a**) (**b**)

Figure 6. Frequency response function (FRF), obtained by sweeping the frequency up and down with the PEH in open-circuit: (**a**) the amplitudes of the voltages applied to the resonant vibration speaker were 3 V and 7 V; (**b**) the amplitudes of the voltages applied to the resonant vibration speaker were 1.5 V and 5 V.

Vibrational energy is pumped between the membrane and the cantilever beam, and for this reason, an accelerometer was mounted at the coupling position. To illustrate the nonlinear dynamics, the acceleration measured in the coupling position was acquired for advanced processing. The first situation investigated was at a sinusoidal wave frequency of 25.4 Hz; Figure 6b is a reference, showing an amplitude of 5 V. The acceleration as a function of time and its Fourier transform are shown in Figure 7a.

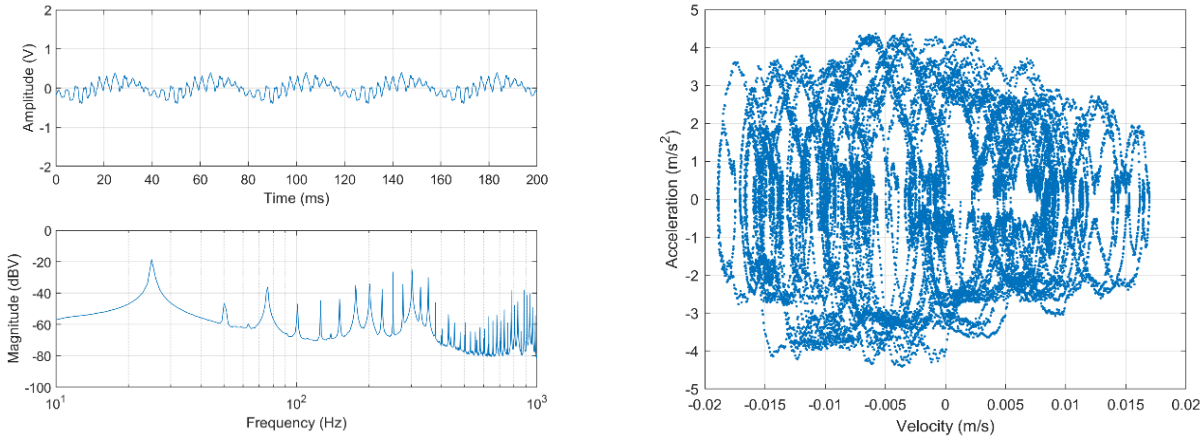

(**a**) (**b**)

Figure 7. PEH is excited by a sinusoidal wave with an amplitude of 5 V and frequency of 25.4 Hz: (**a**) voltage-time response and its Fourier transform; (**b**) experimentally measured phase portrait.

Poly-stable behavior was experimentally demonstrated in this favorable situation for the PEH in terms of harvested energy. In addition, the phase portrait shown in Figure 7b confirms the poly-stable behavior of the proposed deformable structure. To elucidate the behavior of the deformable structure, a new measurement immediately following the resonated peak obtained important information. This very interesting situation occurred immediately after the high vibration amplitude was lost at 25.6 Hz, a distinctive transition for a nonlinear PEH. The experimental results are shown in Figure 8.

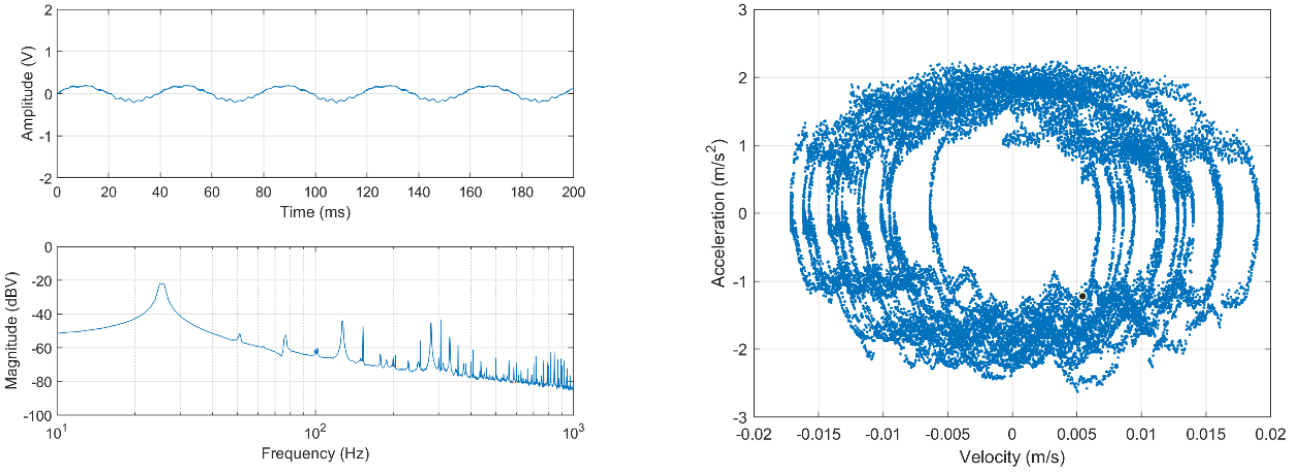

Figure 8. PEH excited by a sinusoidal wave with an amplitude of 5 V and frequency of 25.6 Hz: (**a**) voltage-time response and its Fourier transform; (**b**) experimentally measured phase portrait.

The acceleration as a function of time and its Fourier transform are shown in Figure 8a. The nonlinear behavior of the PEH that is the subject of this research is shown in the phase portrait in Figure 8b. In this situation, the deformable structure remained nonlinear, with behavior specific to a multi-stable PEH.

3.2. Output Power of a Nonlinear Piezoelectric Electrical Harvester

The Norton equivalent circuit of the PEH shown in Figure 9 is a simplified model for calculating the harvester energy.

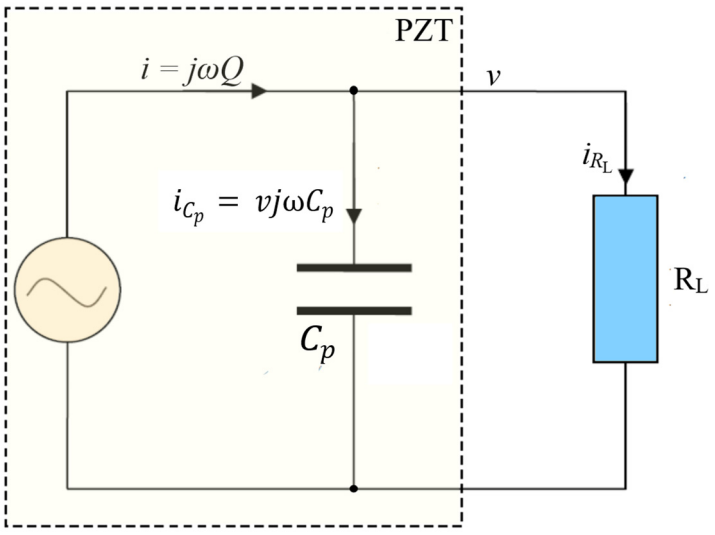

Figure 9. Norton equivalent circuit of a piezoelectric energy harvester.

Applying Kirchhoff's laws to the Norton equivalent circuit of an energy harvester, the power dissipated on the load resistance R_L is calculated as follows:

$$P_{RL} = i_{R_L}^2 R_L = \left(i - i_{C_p}\right)^2 R_L = \left(j\omega Q - vj\omega C_p\right)^2 R_L, \tag{4}$$

where C_p is the static plus dynamic capacitance of piezoelectric material. In Equation (4), P_{RL} is the electrical power delivered to the load resistor. It can be seen that P_{RL} is the function of the load resistance. Its maxima can hence be found using the following calculation:

$$\frac{dP_{RL}}{dR_L} = 0, \tag{5}$$

The result of Equation (5) is the matching condition when $R_L = 1/\omega C_p$ and the power reaches its peak value, which is

$$P_{RLmax} = \frac{\omega Q^2}{2C_p}, \tag{6}$$

The impedance matching condition is fulfilled when the load resistance is equal to the internal impedance of the PEH, and a maximum power will be transferred to the external load. The effect of the dynamic capacitance C_p and the vibration frequency ω on the impedance matching condition can be observed.

To estimate the energy harvesting capacity of the nonlinear PEH, the voltage, current, and power depending on the resistor load were measured and calculated. The voltage, current, and power were investigated under the conditions illustrated in Figure 6b. The nonlinear PEH was in vibration at resonance, and the resonant vibration speaker was excited by a sinusoidal wave with an amplitude of 5 V and frequency of 20.8 Hz. The experimental results are shown in Figure 10.

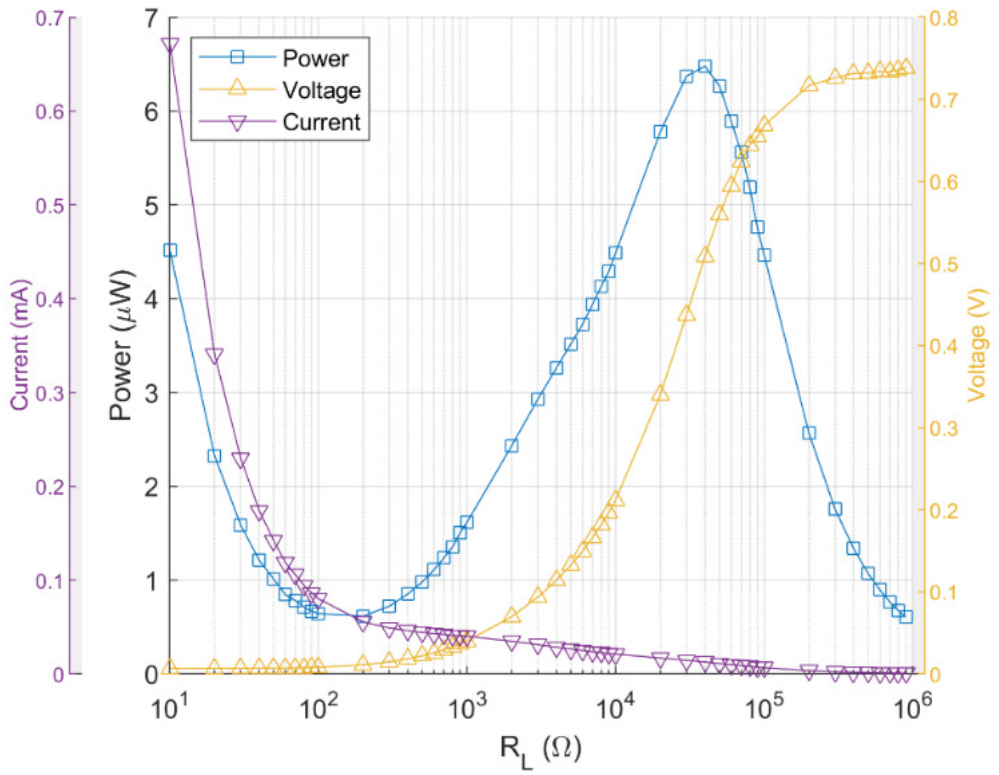

Figure 10. Power, voltage, and current depending on the load resistance value R_L for PEH excited by a sinusoidal wave with an amplitude of 5 V and frequency of 20.8 Hz.

It can be seen that the trend of the experimental data is in good accordance with the above theoretical expectations based on the Norton equivalent circuit described in Figure 9. The voltage increased gradually and was saturated at the open-circuit voltage of about 0.74 Vrms. The current gradually decreased, and the maximum current was at the initial stage, approximately 0.68 mArms. The power increased first, reached a peak value, and then decreased. The measured peak power point was obtained for $R_L \cong 40$ kΩ. The peak power for the optimal value of the load resistor was about 6.8 μWrms, measured immediately before the PEH passed the linear resonance peak. The increase in the power for the load resistance values of less than 100 Ω was due to a shift in the frequency response of the nonlinear deformable structure to lower frequencies when approaching the short circuit condition. This situation is usually avoided in the case of a PEH by restricting the range of the power measurement for load resistance values of 10^3–10^6 Ω.

The maximum power of the nonlinear PEH was obtained by maintaining the identical amplitude of the sinusoidal excitation wave and gradually changing the frequency to 25.4 Hz, as shown in Figure 6b. The experimental results are shown in Figure 11.

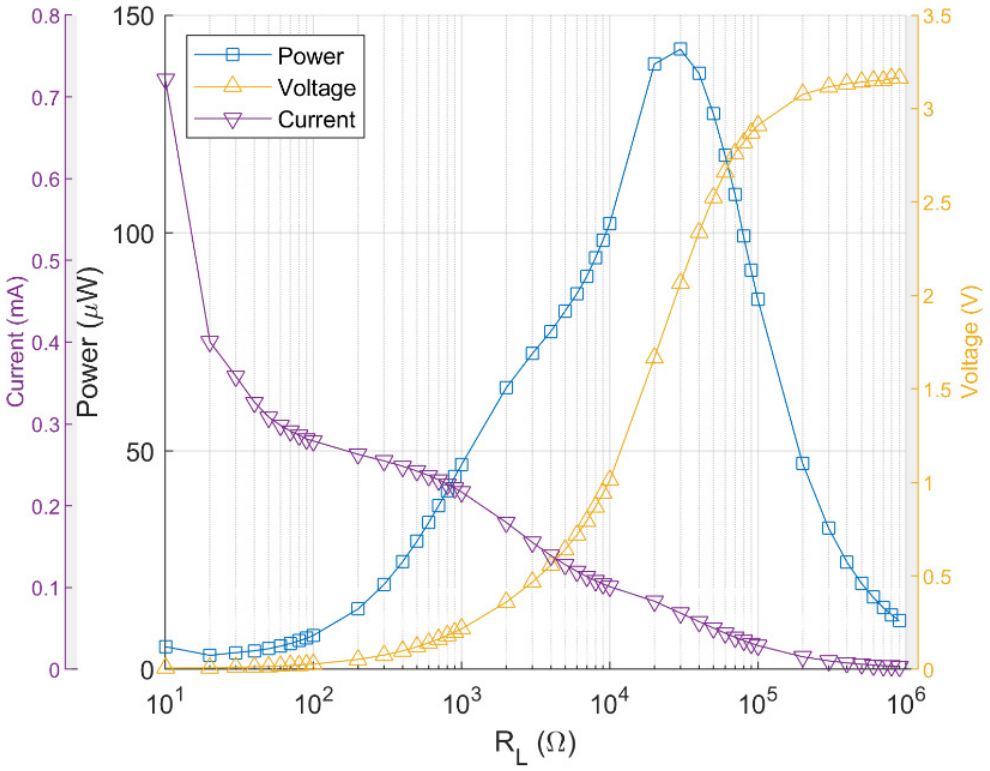

Figure 11. Power, voltage, and current depend on the load resistance value R_L for PEH excited by a sinusoidal wave with an amplitude of 5 V and frequency of 25.4 Hz.

The voltage increased gradually and was saturated at the open-circuit voltage at about 3.2 Vrms. The current decreased gradually and the maximum current was at the initial stage, about 0.72 mArms. The power increased first, reached a peak value, and then decreased. The measured peak power point was obtained for $R_L \cong 30$ kΩ. The peak power at the optimal value of the load resistor was about 0.144 μWrms.

In both of the situations presented above, the power was measured in the unimorph configuration of the PEH to maintain the upper side for the output power mapping measurements. After demonstrating the energy harvesting capacity of nonlinear PEHs, it is necessary to mention its advantages and competitiveness. The main advantage of the nonlinear PEH results from the power generated in the hardening response in Figure 11, which was twenty times higher than the reference power in Figure 10. This nonlinear response provides a broad bandwidth on which power can be harvested relative to the linear PEH

counterparts. When the excitation was provided by a sinusoidal wave with an amplitude of 5 V, the experimental results show a bandwidth of 2.6 Hz or a mistuning capacity of 11% in terms of the natural frequency of the console beam. A frequency bandwidth of 3.0 Hz (12%) was obtained when the excitation is conducted with a sinusoidal wave with an amplitude of 7 V; in this case, the acceleration was equal to 2.5 m/s^2. Nonlinear behavior at a level of only 0.5 m/s^2 is a clear advantage of the proposed nonlinear PEH, and this advantage is combined with an increase in the frequency bandwidth.

3.3. Experimental Output Power Mapping

The output power mapping was obtained using direct experimental measurements for the upper side PZT patch of the PEH, unimorph configuration. The upper side of the PZT was divided into twelve small surfaces, each with a size of 15 mm × 10 mm, as shown in Figure 3b. The output power map for the resistive load of R_L = 40 kΩ was measured experimentally. The resonant vibration speaker was excited with a sinusoidal wave with an amplitude of 5 V and a frequency of 20.8 Hz, i.e., an acceleration equal to 1.2 m/s^2. The harvested energy was concentrated in column C1, as shown in Figure 12a, under the conditions mentioned above.

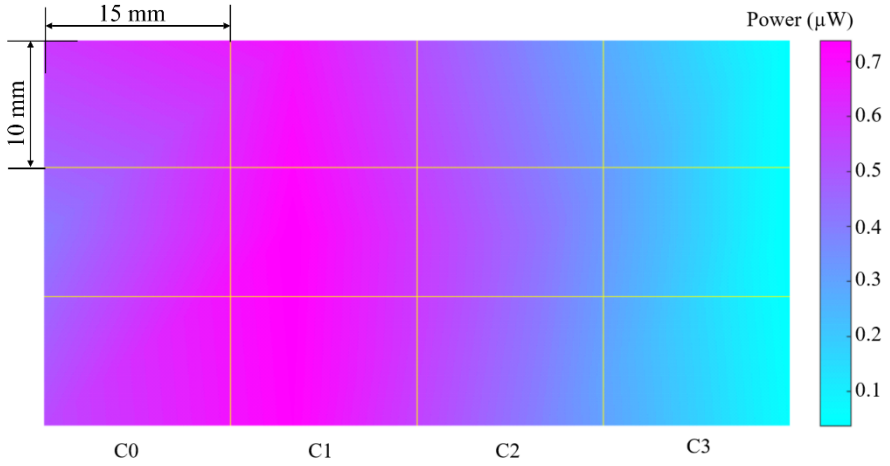

(**a**)

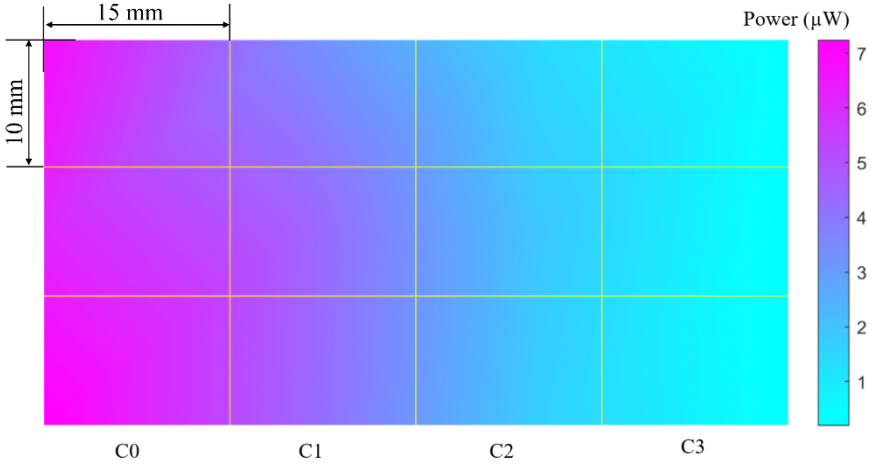

(**b**)

Figure 12. Mapping of the output power of PEH excited by a sinusoidal wave with an amplitude of 5 V and frequency: (**a**) 20.8 Hz and (**b**) 25.4 Hz.

The method of mapping the output power is a time-consuming experiment and difficult to automate without profound changes in the electrical connections that would drastically influence the behavior of PEH. In the present paper, before measuring the power for a new area, the excitation sinusoidal wave was stopped to move the PZT contact. For each area, the identical measuring condition was created using an upward frequency sweep.

The PEH's nonlinear response to a frequency that ensured the maximum deformation of the cantilever beam changed the output power map, as shown in Figure 12b. The harvested energy was concentrated in the C0 column near the fixation armature. The experimental condition was identical from the point of view of the sinusoidal wave amplitude, but the change in frequency at 25.4 Hz generated a new level of acceleration equal to 2.5 m/s^2. In this measurement, the value R_L = 30 kΩ for the resistive load was used as the effect of shifting in the dynamic capacitance. The modification of the output power map was determined by a new distribution of stress/strain in the nonlinear PEH. In an application that was subject to vibrations in the environment, the two situations presented in Figure 12 were encountered at the limit, so that only the C3 column of the PZT patch could be removed. Considering the particular application in which the PEH will operate at a frequency of 25.4 Hz, as in Figure 12b, then columns C2 and C3 of the PZT patch can be removed. These output power maps provide experimental support for the design and implementation of a miniaturized nonlinear PEH. Power maps are a reference in the design process to optimize the size of the PZT patch for a nonlinear deformable structure based on the cantilever beam.

4. Discussion

The most common methods of characterizing piezoelectric energy harvesting are those in which the PEH is mounted on top of the shaker and uses a vibrometer to measure the amplitude of vibrations. The resonance significantly amplifies the amplitude of the vibrations that generate stress/strain for the piezoelectric effect, leading to high energy outputs. The basic measurements have the following procedure: (i) a sweep of the sinusoidal wave frequency is performed for a certain interval in order to find resonance in the open circuit configuration, and (ii) at the resonant frequency, systematic voltage measurements are made to investigate the PEH response in relation to a resistive load (RL).

This study investigated a deformable nonlinear structure consisting of the membrane of a resonant vibration speaker and a cantilever beam connected in a series. The process of energy harvesting is in the charge of the cantilever beam, the sides of which two PZTs are glued to in a parallel bimorph configuration. During vibrations, the loading conditions and the distribution of stress inside the PEH change dramatically due to deformations that lead to a nonlinear rigidity. The equivalent restoring force of a multi-stable PEH is described by a high-order polynomial to shape dynamic behavior. This nonlinear stiffness allows for a wide range of PEH working frequencies, as has been experimentally demonstrated.

The nonlinear PEH is characterized by two different frequency response functions for up and down frequency sweeps. The maximum value of power for matched R_L is the harvested electrical power. Using this method, the PEH is treated as a black box, and this is usually the perfect approach for any type of electric harvesting machine. Experimental measurement of the power map is a difficult and time-consuming task in the case of a nonlinear PEH.

Additional measurements are required to elucidate the behavior of the proposed nonlinear deformable structure, and improved experimental methods must be involved to understand its effects. These investigations will allow for an experimentally validated conclusion in the conditions of excitation with a constant acceleration, independent of the frequency of excitation. This situation is easy to implement in the experimental setup in Figure 4a through a control in the closed loop of the signal generator.

5. Conclusions

In this paper, a nonlinear deformable structure used as a piezoelectric energy harvester is presented. The best achievement of this study is related to the nonlinear response of a very simple deformable structure that combines the membrane of the resonant vibration speaker and the console beam to achieve improved performance of the piezoelectric energy harvester. Its nonlinear behavior was demonstrated by its frequency response function and advanced experimental investigations. Frequency response function, Fourier transform and phase portrait validated a multi-stable nonlinear deformable structure.

The experimental output power map shows that the proposed nonlinear PEH has an energy distribution suitable for the design of compact energy harvesters based on equivalent deformable structures. Nonlinear behavior at moderate vibration acceleration equal to only 0.5 m/s^2 is a clear advantage of the proposed nonlinear PEH, combined with large frequency bandwidth. Two situations to measure the harvested power were chosen to obtain experimental proof of the effect produced by a multi-stable deformable structure. Thus, the harvested power with optimal load resistance in two situations was measured—a reference power of approximately 0.144 μWrms at a frequency of 20.8 Hz and a reference power of 6.8 μWrms at a frequency of 25.4 Hz. The main advantage of the nonlinear PEH was the result of the power generated in the hardening response being twenty times higher than the reference power. The presentation of the most significant experimental results of a nonlinear PEH, followed by the experimental mapping of the output power, provides an image of the electrical performance of the investigated deformable structure.

Funding: This research received no external funding.

Conflicts of Interest: The authors declare no conflict of interest.

References

1. Sezer, N.; Koç, M. A comprehensive review on the state-of-the-art of piezoelectric energy harvesting. *Nano Energy* **2021**, *80*, 105567. [CrossRef]
2. Liang, H.; Hao, G.; Olszewski, O.Z. A review on vibration-based piezoelectric energy harvesting from the aspect of compliant mechanisms. *Sens. Actuators A Phys.* **2021**, *331*, 112743. [CrossRef]
3. Covaci, C.; Gontean, A. Piezoelectric Energy Harvesting Solutions: A Review. *Sensors* **2020**, *20*, 3512. [CrossRef] [PubMed]
4. Bogue, R. Energy harvesting and wireless sensors: A review of recent developments. *Sens. Rev.* **2009**, *29*, 194–199. [CrossRef]
5. Harb, A. Energy harvesting: State-of-the-art. *Renew. Energy* **2011**, *36*, 2641–2654. [CrossRef]
6. Khaligh, A.; Zeng, P.; Zheng, C. Kinetic Energy Harvesting Using Piezoelectric and Electromagnetic Technologies—State of the Art. *IEEE Trans. Ind. Electron.* **2010**, *57*, 850–860. [CrossRef]
7. Daqaq, M.F.; Masana, R.; Erturk, A.; Quinn, D.D. On the role of nonlinearities in vibratory energy harvesting: A critical review and discussion. *Appl. Mech. Rev.* **2014**, *66*, 040801. [CrossRef]
8. Zhu, D.; Tudor, M.J.; Beeby, S.P. Strategies for increasing the operating frequency range of vibration energy harvesters: A review. *Meas. Sci. Technol.* **2009**, *21*, 022001. [CrossRef]
9. Williams, C.; Yates, R.B. Analysis of a micro-electric generator for microsystems. *Sens. Actuators A Phys.* **1996**, *52*, 8–11. [CrossRef]
10. Keshmiri, A.; Wu, N. A Wideband Piezoelectric Energy Harvester Design by Using Multiple Non-Uniform Bimorphs. *Vibration* **2018**, *1*, 93–104. [CrossRef]
11. Edwards, B.; Aw, K.C.; Hu, A.P. Mechanical frequency up-conversion for sub-resonance, low-frequency vibration harvesting. *J. Intell. Mater. Syst. Struct.* **2016**, *27*, 2145–2159. [CrossRef]
12. Kathpalia, B.; Tan, D.; Stern, I.; Erturk, A. An experimentally validated model for geometrically nonlinear plucking-based frequency up-conversion in energy harvesting. *Smart Mater. Struct.* **2017**, *27*, 015024. [CrossRef]
13. Ramlan, R.; Brennan, M.J.; Mace, B.R.; Kovacic, I. Potential benefits of a nonlinear stiffness in an energy harvesting device. *Nonlinear Dyn.* **2010**, *59*, 545–558. [CrossRef]
14. Friswell, M.I.; Ali, S.F.; Adhikari, S.; Lees, A.W.; Bilgen, O.; Litak, G. Nonlinear piezoelectric vibration energy harvesting from a vertical cantilever beam with tip mass. *J. Intell. Mater. Syst. Struct.* **2012**, *23*, 1505–1521. [CrossRef]
15. Erturk, A.; Inman, D.J. An experimentally validated bimorph cantilever model for piezoelectric energy harvesting from base excitations. *Smart Mater. Struct.* **2009**, *18*, 025009. [CrossRef]
16. Stanton, S.C.; Erturk, A.; Mann, B.P.; Inman, D.J. Nonlinear piezoelectricity in electroelastic energy harvesters: Modeling and experimental identification. *J. Appl. Phys.* **2010**, *108*, 074903. [CrossRef]
17. Sebald, G.; Kuwano, H.; Guyomar, D.; Ducharne, B. Experimental Duffing oscillator for broadband piezoelectric energy harvesting. *Smart Mater. Struct.* **2011**, *20*, 102001. [CrossRef]

18. Cottone, F.; Vocca, H.; Gammaitoni, L. Nonlinear energy harvesting. *Phys. Rev. Lett.* **2009**, *102*, 080601. [CrossRef] [PubMed]
19. Mann, B.; Owens, B. Investigations of a nonlinear energy harvester with a bistable potential well. *J. Sound Vib.* **2010**, *329*, 1215–1226. [CrossRef]
20. Triplett, A.; Quinn, D.D. The Effect of Non-linear Piezoelectric Coupling on Vibration-based Energy Harvesting. *J. Intell. Mater. Syst. Struct.* **2009**, *20*, 1959–1967. [CrossRef]
21. Gebrel, I.F.; Wang, L.; Asokanthan, S.F. Dynamic Analysis and Design of a Novel Ring-Based Vibratory Energy Harvester. *Vibration* **2019**, *2*, 271–284. [CrossRef]
22. Sato, T.; Watanabe, K.; Igarashi, H. Coupled analysis of electromagnetic vibration energy harvester with nonlinear oscillation. *IEEE Trans. Magn.* **2014**, *50*, 313–316. [CrossRef]
23. Xie, Z.; Wang, T.; Kwuimy, C.K.; Shao, Y.; Huang, W. Design, analysis and experimental study of a T-shaped piezoelectric energy harvester with internal resonance. *Smart Mater. Struct.* **2019**, *28*, 085027. [CrossRef]
24. Xiong, L.; Tang, L.; Mace, B.R. Internal resonance with commensurability induced by an auxiliary oscillator for broadband energy harvesting. *Appl. Phys. Lett.* **2016**, *108*, 203901. [CrossRef]
25. Xiong, L.; Tang, L.; Mace, B.R. A comprehensive study of 2:1 internal-resonance-based piezoelectric vibration energy harvesting. *Nonlinear Dyn.* **2018**, *91*, 1817–1834. [CrossRef]
26. Saint-Martin, C.; Morel, A.; Charleux, L.; Roux, E.; Benhemou, A.; Badel, A. Power expectation as a unified metric for the evaluation of vibration energy harvesters. *Mech. Syst. Signal. Process.* **2022**, *181*, 109482. [CrossRef]
27. Liao, Y.; Liang, J. Unified modeling, analysis and comparison of piezoelectric vibration energy harvesters. *Mech. Syst. Signal. Process.* **2019**, *123*, 403–425. [CrossRef]
28. Zaghari, B.; Rustighi, E.; Ghandchi Tehrani, M. Improved Modelling of a Nonlinear Parametrically Excited System with Electromagnetic Excitation. *Vibration* **2018**, *1*, 157–171. [CrossRef]
29. Arroyo, E.; Badel, A.; Formosa, F.; Wu, Y.; Qiu, J. Comparison of electromagnetic and piezoelectric vibration energy harvesters: Model and experiments. *Sens. Actuators A Phys.* **2012**, *183*, 148–156. [CrossRef]
30. Le, C.P.; Halvorsen, E.; Søråsen, O.; Yeatman, E.M. Wideband Excitation of an Electrostatic Vibration Energy Harvester with Power-Extracting End-Stops. *Smart Mater. Struct.* **2013**, *22*, 075020. [CrossRef]
31. Janphuang, P.; Lockhart, R.; Uffer, N.; Briand, D.; de Rooij, N.F. Vibrational Piezoelectric Energy Harvesters Based on Thinned Bulk PZT Sheets Fabricated at the Wafer Level. *Sens. Actuators A Phys.* **2014**, *210*, 1–9. [CrossRef]
32. Huang, Y.; Zhao, Z.; Liu, W. Systematic adjustment strategy of a nonlinear beam generator for high-energy orbit. *Mech. Syst. Signal. Process.* **2022**, *166*, 108444. [CrossRef]
33. Morel, A.; Brenes, A.; Gibus, D.; Lefeuvre, E.; Gasnier, P.; Pillonnet, G.; Badel, A. A comparative study of electrical interfaces for tunable piezoelectric vibration energy harvesting. *Smart Mater. Struct.* **2022**, *31*, 045016. [CrossRef]
34. Masana, R.; Daqaq, M.F. Response of duffing-type harvesters to band-limited noise. *J. Sound Vib.* **2013**, *332*, 6755–6767. [CrossRef]
35. Andò, B.; Baglio, S.; Bulsara, A.; Marletta, V.A. Bistable buckled beam based approach for vibrational energy harvesting. *Sens. Actuators A Phys.* **2014**, *211*, 153–161. [CrossRef]
36. Zayed, A.A.; Assal, S.F.; Nakano, K.; Kaizuka, T.; El-Bab, F.; Ahmed, M. Design procedure and experimental verification of a broadband quad-sTable 2-DOF vibration energy harvester. *Sensors* **2019**, *19*, 2893. [CrossRef]
37. Zhou, X.; Gao, S.; Liu, H.; Jin, L. Nonlinear Hybrid Piezoelectric and Electromagnetic Energy Harvesting Driven by Colored Excitation. *Energies* **2018**, *11*, 498. [CrossRef]
38. Hajati, A.; Kim, S.G. Ultra-wide bandwidth piezoelectric energy harvesting. *Appl. Phys. Lett.* **2011**, *99*, 083105. [CrossRef]
39. Huang, D.; Zhou, S.; Litak, G. Theoretical analysis of multi-stable energy harvesters with high-order stiffness terms. *Commun. Nonlinear Sci. Numer. Simul.* **2019**, *69*, 270–286. [CrossRef]
40. Lan, C.; Qin, W. Enhancing ability of harvesting energy from random vibration by decreasing the potential barrier of bistable harvester. *Mech. Syst. Signal. Process.* **2017**, *85*, 71–81. [CrossRef]
41. Ando, B. How can energy be scavenged from wideband vibrations? *IEEE Instrum. Meas. Mag.* **2015**, *18*, 40–44. [CrossRef]